frontiers | Frontiers in Chemical Biology

TYPE Methods
PUBLISHED 30 May 2023
DOI 10.3389/fchbi.2023.1181137

OPEN ACCESS

EDITED BY
Isabel Correia,
University of Lisbon, Portugal

REVIEWED BY
Yiannis Kourkoutas,
Democritus University of Thrace, Greece
Kaiwen Yu,
St. Jude Children's Research Hospital, United States

*CORRESPONDENCE
Xiao-Le Han,
HXL1220@hotmail.com
Yue Sun,
suny@scuec.edu.cn
Lan-Ping Guo,
glp01@126.com
Xiao-Long Yang,
yxl19830915@163.com

†These authors have contributed equally to this work

RECEIVED 07 March 2023
ACCEPTED 20 April 2023
PUBLISHED 30 May 2023

CITATION
Yu F, Han X-L, Zhu J, Dai L, Liu S, Liu Q-P, Yang J, Sun Y, Guo L-P and Yang X-L (2023), A natural product noraucupatin against multidrug-resistant *Enterococcus faecium*: an inhibition mechanism study. *Front. Chem. Biol* 2:1181137. doi: 10.3389/fchbi.2023.1181137

A natural product noraucupatin against multidrug-resistant *Enterococcus faecium*: an inhibition mechanism study

Fan Yu[1†], Xiao-Le Han[1*†], Jiahua Zhu[1], Le Dai[1], Shuzhi Liu[2], Qing-Pei Liu[2], Jian Yang[3], Yue Sun[3*], Lan-Ping Guo[4*] and Xiao-Long Yang[2*]

[1]Key Laboratory of Analytical Chemistry of the State Ethnic Affairs Commission, School of Chemistry and Materials Science, South-Central Minzu University, Wuhan, China, [2]The Modernization Engineering Technology Research Center of Ethnic Minority Medicine of Hubei Province, School of Pharmaceutical Sciences, South-Central Minzu University, Wuhan, China, [3]State Key Laboratory of Separation Membrane and Membrane Process, School of Chemistry, Tiangong University, Tianjin, China, [4]State Key Laboratory Breeding Base of Dao-di Herbs, National Resource Center for Chinese Materia Medica, China Academy of Chinese Medical Sciences, Beijng, China

Background: This work elucidates the antimicrobial activity and mechanism of action of the natural product noraucupatin against MDR *Enterococcus faecium*. *E. faecium* has become a major opportunistic pathogen with the worldwide spread of multidrug-resistant (MDR) isolates, especially vancomycin-resistant *enterococci* (VRE), belongs to "ESKAPE" organisms causing significant problems widely. Hence, there is a pressing need to discover new promising drugs or alternative therapies. Fortunately, we found a natural product noraucupatin ($C_{13}H_{12}O_3$, a biphenyl compound) with "extremely encouraging" anti-clinical drug-resistant bacterial activity isolated from *yeast*-induced *Rowan* suspension cells. A comprehensive and in-depth exploration of antimicrobial mechanisms will bring fresh insights for researchers to develop novel antimicrobial strategies against MDR bacteria.

Methods: The antibacterial effect of noraucupatin against MDR *E. faecium* is investigated from a microbial metabolism perspective using microcalorimetry. The antibacterial effect is determined based on the thermodynamic parameters. Based on spectroscopic techniques, microscopy techniques and confocal scanning laser microscopy with membrane probes, the antibacterial mechanism is elucidated definitely.

Results: Comparing with the IC_{50} of noraucupatin against MDR *Enterococcus faecalis*, MRSA, CRPA, the IC_{50} of noraucupatin against MDR *E. faecium* was just 67.54 μM. The growth rate of MDR *E. faecium* decreases with the increase of concentration of noraucupatin. The bacterial intracellular structure entirely

Abbreviations: BMP, bacterial membrane potential; Calcein-AM, Calcein Acetoxymethyl Ester; CRPA, Carbapenem-resistant *pseudomonas aeruginosa*; CSLM, Confocal scanning laser microscopy; DAPI, 4,6-diamidino-2-phenylindole; DiBAC4[3], Bis-(1,3-dibutylbarbituric acid) trimethine oxonol; ESKAPE, *Enterococcus faecium*, *Staphylococcus aureus*, *Klebsiella pneumonia*, *Acinetobacter baumannii*, *Pseudomonas aeruginosa* and *Enterobacter species*; IC50, inhibitory concentration; MDR *E. faecalis*, MDR *Enterococcus faecalis*; MDR *E. faecium*, MDR *Enterococcus faecium*; MDR, multidrug-resistant; MRSA, Methicillin-resistant *staphylococcus aureus*; OD, Optical density; PI, Propidium Iodide; RRBc, rabbit red blood cells; VRE, vancomycin-resistant *enterococci*.

collapses and the slurries flow out under the influence of high levels of noraucupatin by TEM. The changes of membrane potential, permeability and evidences of nucleic acid leakage was obtained by CSLM and UV, the mechanism of noraucupatin against MDR *E. faecium* we explored.

Conclusion: The present study highlights the excellent antibacterial activity of noraucupatin against MDR *E. faecium* by altering the permeability of the membrane and disrupting the membrane potential leading to electrolyte permeation. In addition, noraucupatin has excellent biocompatibility through its haemolytic activity in rabbit erythrocyte. These findings suggest that noraucupatin could be used in infectious diseases caused by MDR *E. faecium.*

KEYWORDS

a biphenyl compound, MDR *Enterococcus faecium*, membrane potential, antibacterial mechanism, microcalorimetric method

1 Introduction

1.1 Background

With the widespread use of traditional antibiotics, the resistance of bacteria has gradually increased, resulting in considerably resistant bacteria and the emergence of multi-drug resistant (MDR) strains, even super bacteria (da Silva et al., 2022; Zhou et al., 2022). However, the resistance rate of old-fashioned antibacterial drugs such as penicillin, cephalosporin, erythromycin, and azithromycin has even reached 80%–90% (Tan et al., 2018; Murray et al., 2022; Platon et al., 2022; She et al., 2022). Meanwhile, new antibacterial drugs have not been successfully developed. There is no doubt that multidrug resistance, along with the lack of new antimicrobial drugs, has led to a public health crisis (Dai et al., 2022; Zhang and Cheng, 2022). The development of novel chemicals as therapeutic agents against MDR infections is a pressing need.

Enterococcus has two main species (namely, *Enterococcus faecalis* and *E. faecium*) are minority members of the normal flora of the human, regarded as harmless commensal bacteria primarily (Briaud and Carroll, 2020; Li Q. et al., 2022). Currently, they have become major opportunistic pathogens due to considerably higher resistant to antimicrobials, becoming a leading major cause of multidrug-resistant bacterial infections, especially in critically ill and immunocompromised patients with prolonged-course antimicrobial treatments and/or prolonged hospital stays (Ruhal and Kataria, 2021). Moreover, some stains of *Enterococcus faecium* have developed strong levels of resistance to ampicillin, vancomycin and aminoglycosides, which are three of the traditionally most useful anti-*enterococcal* antibiotics, being a significant danger and pose a risk to public health (Kessel et al., 2021). While studies have revealed that there are newer antibiotics such as linezolid, daptomycin and tigecycline with superior *in vitro* activity against enteric isolation, the success rate of clinical use has also been reduced by the emergence of resistance (Tran et al., 2015; Smith et al., 2018; Yi et al., 2022). It goes without saying that the current antibacterial drugs to treat MDR *E. faecium* infections are urgently needed. Recently, substituted benzoyl guanidine compounds have been used as lead structures for the discovery of other promising drugs in both synthetic and medicinal chemistry. Peng's group investigated the antimicrobial activity of a different substituted benzene guanidine analog, isopropyl benzene guanidine, against *Enterococci* (Zhang et al., 2019). Carter's group found 1,2,4-oxadiazoles are active against a range of MDR *E. faecium*, including isolates that display susceptibility to vancomycin and daptomycin (Carter et al., 2018). Ribeiro et al. isolate and identified nine compounds from Clusia burlemarxii (Clusiaceae), showed significant activity against tested Gram-positive bacteria, none activity against tested Gram-negative bacteria and fungi (Ribeiro et al., 2011). In the course of literature research, we found that most studies only in term of antimicrobial activity, but did not discuss from the depth of the mechanism of action. Issues such as unclear target, unclear mechanism of action, etc. have emerged as key bottlenecks to be addressed in the study of natural product draggability.

In the previous study, our group isolated a new biphenyl compound, from the suspension cells of Sorbus induced by yeast extract, named noraucupatin (Figure 1, molecular formula is $C_{13}H_{12}O_3$) (Gao et al., 2021). As we know, biphenyl is an essential intermediate in organic chemistry (Jain et al., 2017). The functionalized biphenyl compounds are endowed with pharmacologically significant active groups, which is great potential for forming new active compounds to against MDR-bacteria (Li H. et al., 2022). After activity screening, we found noraucupatin have significantly inhibited effects on MDR *E. faecium*. We have proposed that the antibacterial mechanism is due to the modification of the membrane potential by the substitution of bacterial surface ions. Moreover, sodium influx damages the functional membrane potential, resulting in enhanced permeability of the bacterial membrane. Finally, it destabilizes the membrane structure, making the penetration of electrolytes and genetic material a new way to achieve its antibacterial function.

Here, the antibacterial effect of noraucupatin against MDR E. faecium is investigated from a microbial metabolism perspective using microcalorimetry. The antibacterial effect is determined based on the thermodynamic parameters. Subsequently, we focus on the mechanism of action of noraucupatin against MDR *E. faecium*. Based on spectroscopic techniques, microscopy techniques and confocal scanning laser microscopy with membrane probes, the antibacterial mechanism described in

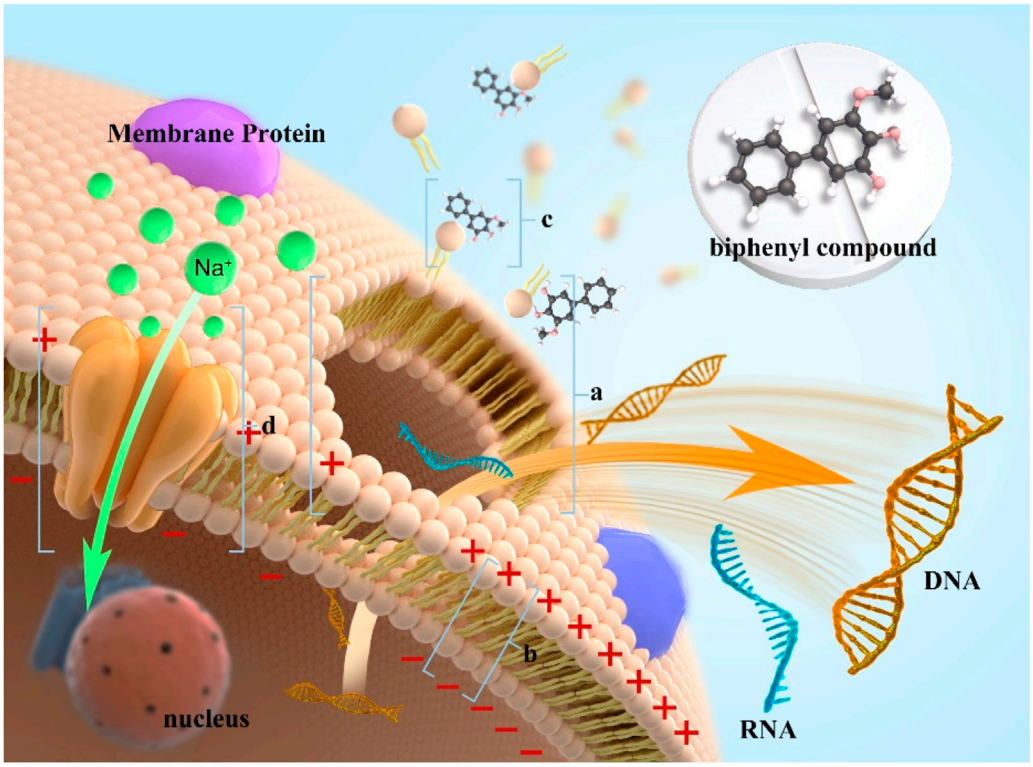

SCHEME 1
Schematic of the antibacterial mechanism of noraucupatin against on MRD *E. faecium*. [**(A)** collapse of cell membrane due to damage to membrane potential; **(B)** It represents a decrease in membrane potential; **(C)** It represents Noraucupatin interacts with the cell membrane; **(D)** It represents the sodium channel.)

Scheme 1 is more definitely elucidated. These findings demonstrate that noraucupatin can significantly inhibit the growth of MDR *E. faecium* and may be a potential therapeutic agent for clinical use. A comprehensive and in-depth exploration of antimicrobial mechanisms will bring fresh insights for researchers to develop novel antimicrobial strategies against MDR bacteria.

2 Methods

2.1 Microbial strains

MDR *E. faecium*, MDR *E. faecalis*, MARS and CRPA were provided by the Modernization Engineering Technology Research Center of Ethnic Minority Medicine of Hubei Province, School of Pharmaceutical Sciences, South-Central University for Nationalities (Wuhan, PR China). LB medium was used for bacteria culture.

2.2 Preparation of compounds

The noraucupatin have been successfully synthesized and characterized (Gao et al., 2021). ^{1}H-NMR and ^{13}C-NMR characteristic spectra of Noraucupatin are detailed in the support information Supplementary Figure S1.

2.3 Microthermal experiment

Microcalorimeters are widely used to obtain thermodynamic and dynamical information about how bacteria grow in response to drugs (Bravo, 2022; Sigg et al., 2022). Briefly, the ampoule method was used for a microcalorimeter with a constant temperature. Before the experiment, all experimental bacteria were incubated in fresh LB medium for 8 h at a dose of 1/1000 before primary culture. And then the cultured bacteria were divided every 5 mL into 8 ampoules, which is with different concentration of noraucupatin (0, 1.85, 3.71, 7.41, 14.82, 29.63, 59.25, 118.51 μM), respectively. Following this, all the ampoules were sealed and thoroughly shaken. Transfer the ampoules to an isothermal microcalorimeter. The thermodynamic curves are recorded after the calorimeter system has been stabilized.

2.4 UV spectrophotometric method

Absorbance was measured by ultraviolet spectrophotometer (UV-3900H) as follows: MDR *E. faecium* in the exponential growth phase were cultured with different concentrations of noraucupatin (0, 7.14, 59.25 μM) incubated at 37°C, 180 rpm for 8 h. Thereafter, MDR *E. faecium* were washed by centrifugation (4,000 rpm, 10 min) and harvested, redistributed on PBS (pH = 7.4). The absorption was recorded at 600 nm for UV absorption.

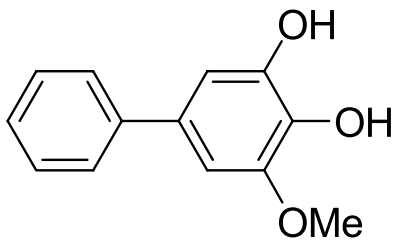

FIGURE 1
Chemical structure of biphenyl compound noraucupatin. The molecular formula is $C_{13}H_{12}O_3$.

2.5 Transmission electron microscope (TEM)

MDR *E. faecium* in the exponential growth phase (activated for 2 h) were cultured with different concentrations of noraucupatin (0, 7.14, 59.25 μM) incubated at 37°C, 180 rpm for 6 h. After incubation, the suspension was centrifuged at 4,000 rpm for 10 min and washed with PBS buffer, and then, prefixed in 2 mL of aldehyde fixative (2.5% glutaraldehyde) for 24 h, photographed using a transmission electron microscope (H-70000FA).

2.6 Confocal laser scanning microscopy (CLSM)

MDR *E. faecium* in the exponential growth phase (activated for 2 h) were cultured with different concentrations of noraucupatin (0, 7.14, 59.25 μM) incubated at 37°C, 180 rpm for 6 h. After incubation, the suspension was centrifuged at 4,000 rpm for 10 min and washed with PBS buffer, and then, adding fluorescent nuclear probe (Calcein-AM, propidium iodide, DAPI, SYTOX Green reagent) respectively, incubated for 20 min. Ultra-high-resolution laser confocal microscope (LSM900) was used to image the samples on the patch at excitation wavelengths of 535 nm for PI, 494 nm for Calcein-AM, 360 nm for DAPI and 480 nm for SYTOX Green, respectively.

2.7 Membrane potential measurement

The membrane potential sensitive fluorescent probe DiBAC4 [3] (1 μM) was added to MDR *E. faecium* incubated with different concentrations of noraucupatin (0, 1.85, 7.14, 29.63, 59.25, 118.51 μM). After incubation at 37°C, the fluorescence values of the samples were detected at the excitation wavelength of 492 nm and the emission wavelength of 515 nm, respectively. The results were corrected by subtracting the background fluorescence.

2.8 Membrane permeability measurement

To confirm membrane permeability changes, inner membrane permeability was measured by measuring the b-galactosidase activity of MDR *E. faecium* at 37°C using ONPG as a substrate (Jia et al., 2018; Li et al., 2019). MDR *E. faecium* in the exponential growth phase (activated for 2 h) were cultured with different concentrations of noraucupatin (0, 7.14, 59.25 μM) incubated at 37°C, 180 rpm for 6 h. And then 1 mL suspension was taken from the medium per hour as a sample, 0.05 mol L^{-1} ONPG was added, sonicated in an ice bath, and precipitated by centrifugation (4,000 rpm, 10 min). Supernatants were collected and o-nitrophenol formation was measured at 400 nm to monitor membrane permeability of MDR *E. faecium*.

2.9 Nuclear leakage measurement

To confirm the functional damage caused by noraucupatin to the MDR *E. faecium* membrane, electrolyte leakage was measured using a spectrophotometer, as described previously (Rajasekaran et al., 2019; Tao et al., 2021). MDR *E. faecium* in the exponential growth phase (activated for 2 h) were cultured with different concentrations of noraucupatin (0, 7.14, 59.25 μM) incubated at 37°C, 180 rpm for 6 h. And then, 1 mL suspension was taken from the medium per hour and precipitated by centrifugation (4,000 rpm, 10 min). The supernatant was appropriately diluted and the optical density at 260 nm was recorded.

2.10 Hemolytic activity measurement

The hemolytic activity of noraucupatin is determined by the amount of hemoglobin released by the rabbit erythrocytes (Hajtuch et al., 2021; Nazir et al., 2022). Fresh rabbit red blood cells (RBCs) were centrifuged at 3,000 rpm for 10 min, washed three times with sterile PBS, and resuspended in PBS. Then, different concentrations of noraucupatin (0, 1.85, 7.41, 29.63, 118.51 μM) were added and mixed with red blood cells and incubated at 37°C for 60 min. After incubation, the erythrocyte suspension was centrifuged at 3,000 rpm for 3 min, and the absorbance of the supernatant at 576 nm was measured after proper dilution. 2% Triton X-100 and PBS were used as positive and negative controls, respectively (Koh et al., 2013). The hemolysis was calculated using the following formula:

$$\text{Hemolysis\%} = \frac{\text{Mixture}_{576\,\text{nm}} - \text{Negative control}_{576\,\text{nm}}}{\text{Positive}_{576\,\text{nm}} - \text{Negative control}_{576\,\text{nm}}}$$

3 Results

3.1 The investigation of antibacterial properties of noraucupatin

3.1.1 Determination of antibacterial effect by thermodynamic and kinetic parameters

To evaluate the antibacterial effect of noraucupatin, the heat of bacterial growth was monitored in real time by using a microcalorimeter (TAM air) and a power-time curve was drawn. Figure 2A shows the thermogenic curve of the growth process of MDR *E. faecium* without noraucupatin as a control, revealing the four phases of MDR *E. faecium*, namely, the stagnation phase, the exponential phase, the steady phase, and the fading phase. After

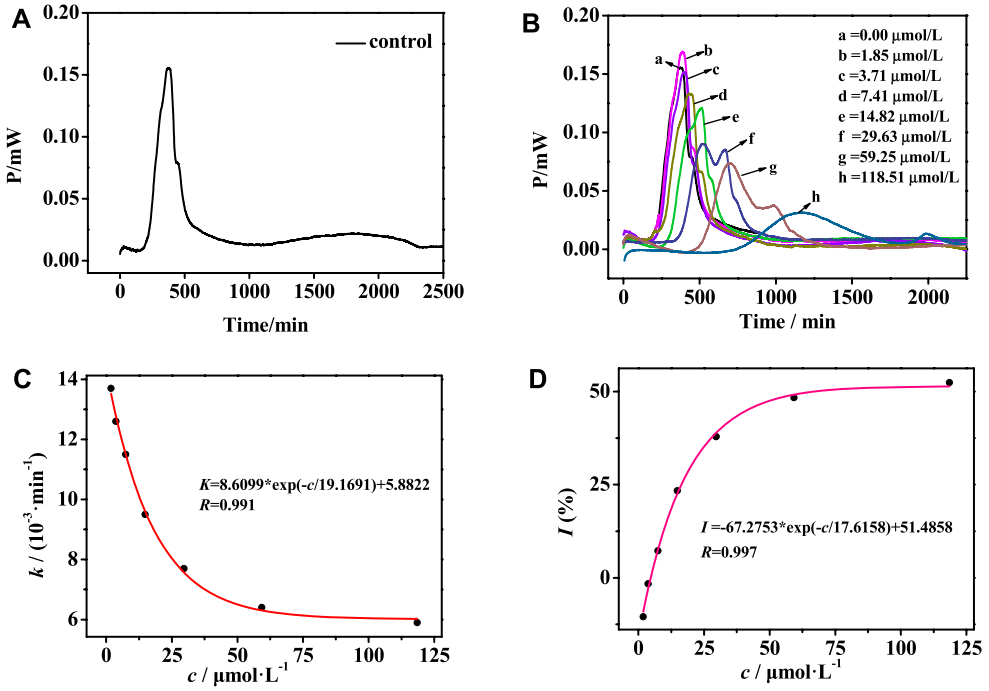

FIGURE 2
(A) Growth thermogenic curves of MDR *E. faecium* without noraucupatin and **(B)** with different concentrations of noraucupatin at 37°C; **(C)** The relationship between different concentrations of noraucupatin and the growth rate constant *k*; **(D)** Fitting graph of the relationship between noraucupatin concentration and inhibition ratio *I*

TABLE 1 Thermal dynamic parameters of MDR. *E. faecium* growth at different concentrations of noraucupatin.

noraucupatinc [μmolL^{-1}]	*K* [10^{-3}min^{-1}]	*R*	P_m [mW]	Q_{total} [J]	*I* [I%]	IC_{50} [μmolL^{-1}]
0	12.4	0.992	0.155	3.6	0	67.54
1.85	13.7	0.993	0.169	3.5	−10.48	
3.71	12.6	0.997	0.150	2.7	−1.62	
7.41	11.5	0.993	0.133	2.6	7.26	
14.82	9.5	0.991	0.124	2.8	23.38	
29.63	7.7	0.998	0.091	2.2	37.90	
59.25	6.4	0.999	0.074	2.2	48.38	
118.51	5.9	0.996	0.033	2.0	52.41	

incubation with different concentrations of noraucupatin, the thermogenic curve of MDR *E. faecium* changes periodically with increasing concentration of noraucupatin, showing Figure 2B. It follows that the metabolism of MDR *E. faecium* is affected by noraucupatin. To be specific, the low concentration (1.85 μM) induced a stress response of MDR *E. faecium*. Overall, the growth peak of MDR *E. faecium* is lagged and gradually decreases with increasing noraucupatin concentration. When the concentration of noraucupatin reached 118.51 μM, the inhibition rate was more than 50%. All the information indicates that noraucupatin has a significant inhibitory effect on the metabolic growth of MDR *E. faecalis*. How to quantify the inhibitory effect of noraucupatin against MDR *E. faecium*? Depending on the relevant thermodynamic and kinetic parameters calculated from Eq.1. The relevant results are listed in Table1.

$$P_t = P_0 \exp\ (kt)$$

Or

$$\ln P_t = \ln P_0 + kt \quad (1)$$

Here P_t is the thermal power output at time t, P_0 is the thermal power output at time t = 0, and *k* is the growth rate constant. By using linear regression of lnP_t vs. t, the growth rate constant *k* of MDR *E. faecium* can be obtained, showing a clear effect on the

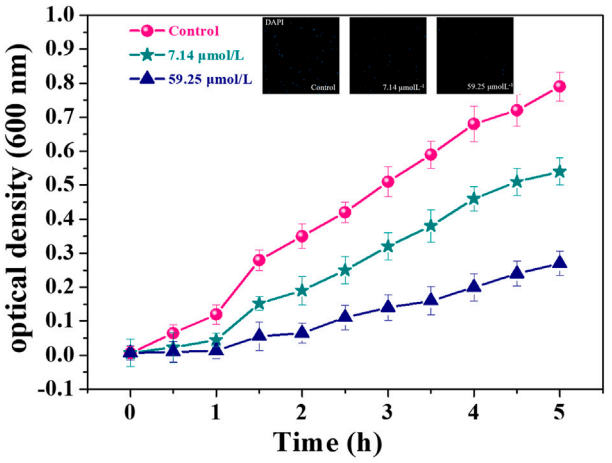

FIGURE 3
OD_{600} value of MDR *E. faecium* with different noraucupatin concentrations. (●blank group; ★ the noraucupatin concentration is 7.14 μM; ▲the noraucupatin concentration is 59.24 μM; the inset is a laser confocal image stained with DAPI).

metabolic growth of MDR *E. faecium*. In addition, the growth rate constant k of *E. faecium* was fitted to the concentration of noraucupatin, as shown in Figure 2C, revealing an excellent exponential relationship. At the same time, the inhibition ratio I and the half-inhibition concentration IC_{50} are then calculated according to Eq. 2. As known to all, the half inhibitory concentration (IC_{50}) is commonly used to characterize the inhibitory ability of the inhibitor in bacterial experiments, referring to the concentration of the inhibitor required to inhibition ratio I is 50% (Bag and Ghorai, 2016).

$$I = \left[\frac{k_0 - k_c}{k_0}\right] \times 100\% \quad (2)$$

where I is the rate of inhibition, k_0 is the rate constant for the control, and k_c is the rate constant for microorganisms inhibited by the inhibitor at concentration c. The growth rate (k) of MDR *E. faecium* decreases with the increase of concentration of noraucupatin, along with inhibition rate (I) gradually increases. The inhibitory rate is a particularly important parameter to demonstrate the inhabit effect of Noraucupatin. Furthermore, when the inhibition rate I is 50%, the obtained concentration of noraucupatin is the half-inhibitory concentration (IC_{50}). The smaller the value of IC_{50}, the stronger its inhibitory activity. Comparing with the IC_{50} of noraucupatin against MDR *E. faecalis* (321.08 μM), MRSA (104.81 μM), CRPA (2640.1 μM), the IC_{50} of noraucupatin against MDR *E. faecium* was only 67.54 μM (shown support information Supplementary Table S1), which showed an excellent inhibit effect. In addition, a positive correlation was observed between drug concentration and thermal effect, while most of the bacterial thermal effect was derived from cell proliferation, indicating that noraucupatin had a significant inhibitory effect on the cell proliferation of MDR *E. faecium* due to the disruption of metabolism (shown support information Supplementary Figures S2–S4). In order to verify the clinical potential of noraucupatin, we tested its antibacterial effects against the traditional medicine ciprofloxacin (shown Supplementary Figures S5–S8), including the antibacterial effect of ciprofloxacin against all the experimental bacteria. Through data analysis, a series of thermodynamic parameters were obtained and listed in Support information Supplementary Tables S2, S3. Comparing by IC_{50} of ciprofloxacin against MDR *E. faecium* (3.0 μM), MDR *E. faecalis* (0.86 μM), MRSA (1.15 μM), CRPA (1.38 μM), noraucupatin shows excellent antibacterial properties, expected to become a new saviour for the treatment of clinical infections caused by drug resistance.

3.1.2 Determination of antibacterial ability by bacterial density method

Optical density (OD) method is often used to quantitatively analyze the sensitivity of microorganisms to antibiotics (Lee et al., 2012). Figure 3 shows the OD growth curves of MDR. *E. faecium* incubated with different concentrations of noraucupatin. The blank group showed the natural growth curve of MDR *E. faecium* and there was an obvious rising point when the growth time reaches 2 h, which was due to the bacteria reached the logarithmic phase growth at this time. The growth inhibition of this bacterial strain is dose-dependent. Under the action of low concentration noraucupatin, the bacterial density OD_{600} changed from 0.72 in blank group to 0.54, and then changed to 0.27 (under the action of high concentration), which demonstrated antibacterial ability increased with noraucupatin concentration. At the same time, the Confocal laser scanning microscopy illustration under DAPI reagent staining also verified our experimental results.

3.2 The exploration of inhibition mechanism of noraucupatin against MDR *E. faecium*

3.2.1 Morphological changes of bacteria

Bacterial morphology changes are the key breakthrough points in the study of bacteriostatic mechanism (Assis et al., 2022; Cylke et al., 2022; Dos Santos et al., 2022). Ultrathin sectioning and transmission electron microscopy were employed to investigate the subsection and shape of the membrane of MDR *E. faecium* incubated with noraucupatin to explore the action of noraucupatin against MDR *E. faecium* at different concentrations. The normal morphology of MDR *E. faecium* without noraucupatin was observed and shown in Figure 4A, which is spherical with clear intact cell wall structure and uniform cytoplasmic staining. After treatment with low concentration of noraucupatin, MDR *E. faecium* organisms were uneven in size and lightly stained, and the cell wall structure began to relax, thinning or even cracking (yellow arrows mark) shown in Figure 4B. Nevertheless, under the influence of high levels of noraucupatin, the bacterial intracellular structure entirely collapses and the slurries flow out (green arrows mark), showing vacuolated irregular circles (shown in Figure 4C). Meanwhile, it was found that noraucupatin molecules were adsorbed to the cell wall to a certain extent (pink arrow mark). All the results demonstrated that bacteriostatic level depended on the dosage of noraucupatin, positively correlated with the damage degree of morphology of MDR *E. faecium*. We speculated that the mechanism of noraucupatin against MDR *E. faecium* was due to the interaction between noraucupatin and the bacterial membrane, resulting in rupture of the membrane and the death of the MDR *E. faecium*.

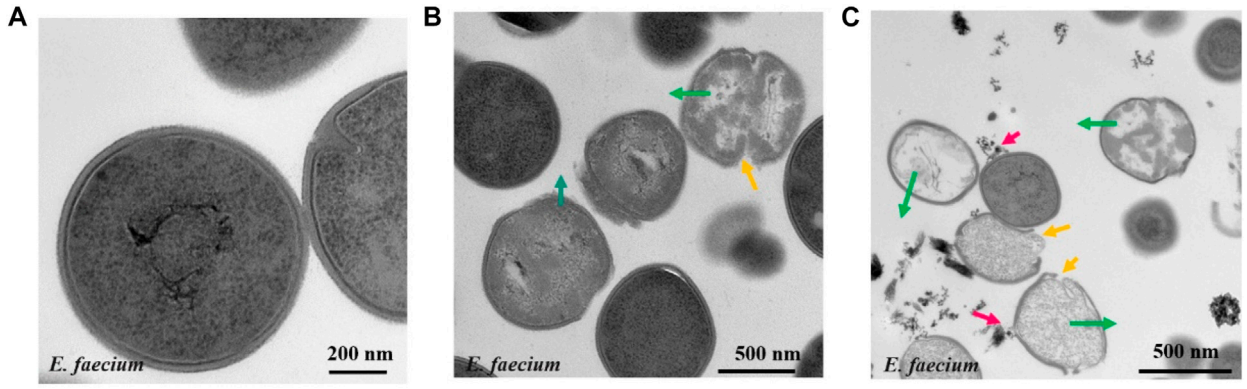

FIGURE 4
Ultrathin electron microscope image of MDR *E. faecium* treated with different noraucupatin concentrations after incubation for 6 h **(A)** without noraucupatin; **(B)** with 7.14 μM noraucupatin; **(C)** with 59.25 μM noraucupatin. Pink arrow shows noraucupatin interacting with the bacterial membranes; Yellow arrow shows film rupture; Green arrow shows cytoplasmic leakage.

3.2.2 Visualization of damage of bacterial membranes

In order to study the damage of bacterial membrane, we studied the permeability of membrane structure by Confocal scanning laser microscopy (CSLM) and Ultraviolet light absorption photometer qualitatively and quantitatively (Pisano et al., 2021; Li H. et al., 2022; Chen et al., 2022). PI (Propidium Iodide) is a membrane impermeable dye, being used as a fluorescent probe to detect membrane damage (Gregorchuk et al., 2022; Lesnichaya et al., 2022). Here's how it works. PI can enter the dead bacteria through the damaged bacterial membrane and intercalate into the DNA double helix of the bacteria, producing red fluorescence. Therefore, observing red fluorescence under fluorescence microscopy is the best evidence for a broken cell membrane. Figures $5A_4$, B_4, C_4 show the bright field of MDR. *E. faecium* at different concentrations of noraucupatin. Fortunately, we truly observed red fluorescence in dark field from MDR *E. faecium* exposure at both low (7.14 μM) and high (59.25 μM) concentration of noraucupatin, shown in Figures 5B, C, respectively. Meanwhile, we used another fluorescent probe (Calcein-AM) which works in the opposite way of PI, to detect live MDR *E. faecium* treated in the same way. As a live cell dye, Calcein-AM can penetrate bacterial membranes and undergo esterase action to remove the AM group, resulting in Calcein that can be detected as green fluorescence in fluorescence microscopy. Almost no red fluorescence was observed in untreated bacteria (Figure $5A_1$), but significant green fluorescence was observed, as shown in Figure $5A_2$. Nearly no green fluorescence was observed in any of the treated bacteria, as shown in Figure $5B_2$, C_2. However, red fluorescence was observed in the bacteria treated by noraucupatin shown in Figures $5B_1$, C_1. Furthermore, according to overlapping of fluorescent signals of PI (red) and Calcein-AM (green) shown in Figure $5B_3$, C_3, it is proved again that a slight amount of noraucupatin can quickly destroy the bacteria membrane, which was mostly destroyed at high concentrations. In addition, we also used fluorescent probes (DAPI and SYTOX green) for quantitative analysis. DAPI can penetrate the entire cell membrane, strongly bind to bacterial DNA, and produce blue fluorescence. SYTOX green is a green nucleic acid dye that easily penetrates the damaged cell, but not the living cell. As shown in Supplementary Figure S9, green fluorescence was observed for SYTOX green staining at both low and high concentrations, while almost no green fluorescence was observed for untreated bacteria. At the same time, the microscopic images under DAPI staining showed a gradual decrease of the blue fluorescent group with increase noraucupatin concentration, indicating gradually decrease in the bacterial density of MDR *E. faecium*. Based on the above conclusions, we conclude that noraucupatin destroys not only the bacterial membrane, but also destroys the bacterial proliferation capacity.

3.2.3 Effect of noraucupatin on membrane potential

The bacterial membrane potential (BMP) is one of the most critical parameters to evaluate the uptake and bactericidal efficacy for the antibacterial agent (Wu et al., 2016; Assis et al., 2022). As the bacterial membrane is damaged, depolarizing and hyperbolizing reactions occur, which are attributed to changes in the concentration of ions in the bacterial cell and a partial loss of bacterial membrane function, causing the membrane to rupture. Therefore, we quantitatively analyze the bactericidal efficacy of noraucupatin against MDR *E. faecium*, which depends on the BMP information of MDR *E. faecium*. From Figure 6C, we can see the change in BMP for MDR *E. faecium* treated with different concentrations of noraucupatin. The reduced membrane potential depends on the Noraucupatin concentration compared to the control. When the concentration of noraucupatin reached 118.51 μM, the membrane potential MDR *E. faecium* decreased by 71%. The noraucupatin has been shown to have excellent uptake and bactericidal efficacy. We infer that the antibacterial mechanism is due to depolarization of the bacterial membrane, inducing a reduction of the membrane potential, which may ultimately lead to irregular bacterial metabolism and death.

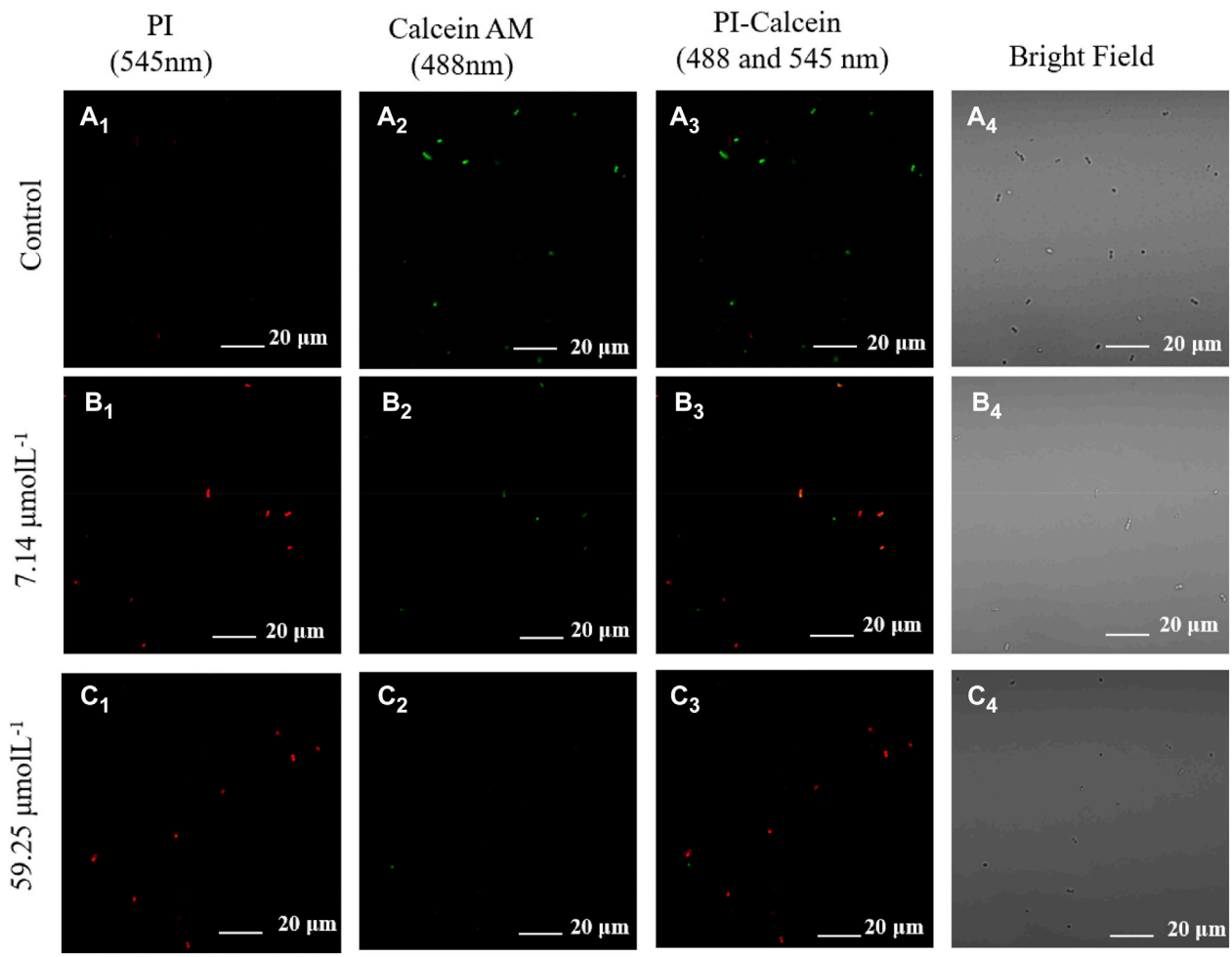

FIGURE 5
Confocal fluorescence images of live and dead MDR *E. faecium* using Calcein AM stain (green fluorescence) and PI stain (red fluorescence) incubated for 5 h without noraucupatin **(A)** and with **(B)** 7.14 μM noraucupatin and with **(C)** 59.25 μM noraucupatin. (Corner mark 1 represents the confocal image at the 545 nm excitation wavelength of the dead bacteria nuclear dye red (PI); Corner mark 2 represents the confocal image at the excitation wavelength of 488 nm for the live bacteria nuclear dye green (Calcein AM); Corner mark 3 indicates confocal images at dual excitation; Corner mark 4 represents the bright field of CLSM.

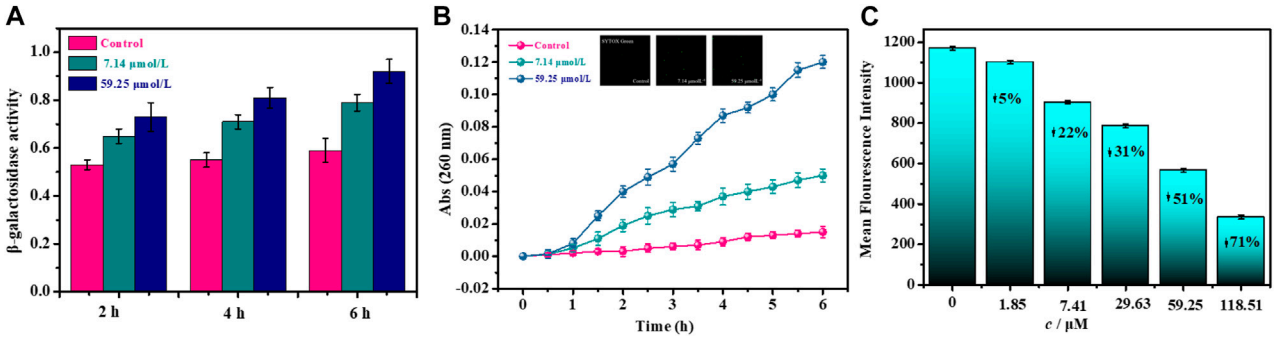

FIGURE 6
Effects of noraucupatin on membrane potential **(A)**, membrane permeability **(B)** and nuclear leakage of MDR *E. faecium* **(C)**. (The inset of B is a laser confocal image stained with SYTOX Green).

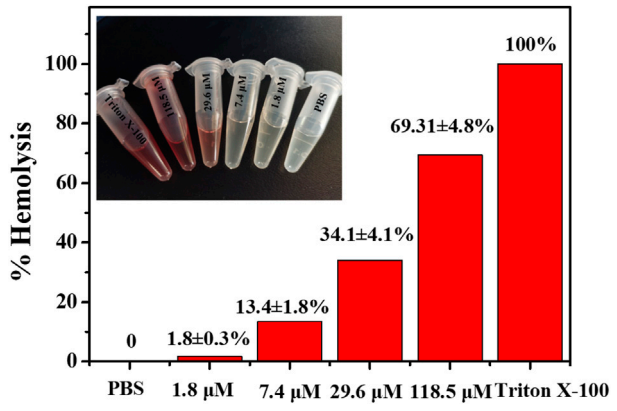

FIGURE 7
Selectivity studies using rabbit red blood cells. The hemolytic effect of noraucupatin under inhibitory concentration gradients was tested. PBS, no hemolytic indicator; Triton X-100 (2%), 100% hemolytic indicator.

3.2.4 Effect of noraucupatin on permeability of membrane

In order to further explore the antibacterial mechanism of noraucupatin, we examined the inner membrane permeability of MDR *E. faecium* treated with different concentration of noraucupatin by measuring the β-galactosidase activity of MDR *E. faecium* at 37°C using ONPG as a substrate (Li et al., 2019). We examined the ability of Noraucupatin to penetrate the inner membrane (plasma membrane) of MDR *E. faecium* by measuring β-galactosidase activity employed UV absorption at 260 nm. The more leakage of β-galactosidase from bacterial cell, the worse the damage of the inner bacterial membrane (Fralliciardi et al., 2022). As shown in Figure 6A, we found that the β-galactosidase activity of untreated MDR *E. faecium* did not change significantly, but gradually increased over incubated time. However, the β-galactosidase activity of MDR *E. faecium* treated with noraucupatin at 7.41 and 59.25 μM respectively increased significantly with the increase of noraucupatin concentration and time of treatment, which indicated that the membrane permeability of MDR *E. faecium* was significantly improved by noraucupatin, and then cell was ruptured.

3.2.5 Effect of noraucupatin on nucleic acid leakage

To further investigate the integrity of the membrane, the release of intracellular components was detected. It is well known that once a bacterial membrane breaks, all of the plasma within it flows out, including small ions such as potassium and phosphate that leach out first, followed by larger molecules such as DNA, RNA and other substances. Among them, nucleotides can be detected by UV-Vis spectrophotometer, having strong UV absorption at 260 nm and called "260 nm absorbing materials" (Hao et al., 2009; Rajasekaran et al., 2019). The UV absorption at 260 nm for MDR *E. faecium* treated with different concentrations of noraucupatin (0, 7.14, 59.25 μM) was measured. We plot the absorbance versus incubation time shown in Figure 6B. For the control group, the absorbance value does not change with the incubation time and approaches zero. In contrast, the absorbance values of the treated group increased significantly with noraucupatin concentration and incubation time, which also indicates the degree of cell membrane rupture.

3.2.6 Hemolytic activity

As a potential antibiotic lead compound with excellent antimicrobial properties, evaluation of cytotoxicity and biocompatibility is necessary. The cytotoxicity of noraucupatin was assessed by analyzing the hemolytic activity on rabbit red blood cells (RRBc). At low concentrations of 1.8 and 7.4 μM, noraucupatin showed low hemolytic activity. As shown in Figure 7, hemolysis increases with varying noraucupatin concentrations. At the highest concentration tested (118 μM), noraucupatin induced 69% hemolysis. It was shown that noraucupatin has relatively low cytotoxicity and is biocompatible.

4 Discussion

In prokaryotes, the function of the bacterial membrane not only maintains a certain shape of the cell and protects the cell, but also participates in the metabolism, the exchange of substances inside and outside the cell, the synthesis of structural macromolecules, and the secretion of numerous enzymes required for life (Mehta et al., 2021; El-Atrees et al., 2022). Therefore, the integrity of the cell membrane is extremely crucial for bacterial growth. However, all the information from damage of morphology, changes in membrane potential, membrane permeability increases and nucleic acid leakage has proved that noraucupatin resistance to MDR *E. faecium* is mainly due to the change and destruction of bacterial membrane properties which may attach the outer membrane of MDR *E. faecium* through electrostatic interactions. We believe that the superior antibacterial activity is due to the chemical structure of noraucupatin, a phenolic compound, which is negatively charged (Lima et al., 2019; Kachur and Suntres, 2020). It has been concluded that the accumulation of hydrophobic phenol groups in lipid bilayers may impair lipid protein interactions, increase membrane permeability, and additionally lead to changes in membrane structure that accelerate the leakage of a large number of components within the cell and ultimately impair membrane integrity (Kachur and Suntres, 2020; Tague et al., 2021). In addition, the hydroxyl group of noraucupatin compounds and the presence of the delocalized electronic system (double bond) enable noraucupatin to act as a proton exchanger depolarizing the cell membrane (Bhattacharya et al., 2018; Kachur and Suntres, 2020). The changes in membrane potential (depolarization and hyperpolarization) are early indicators of bacterial damage. The depolarization phenomenon is mainly caused by changes in pH or increased movement of ions (especially Na^+, K^+). As known to all, these ions (especially Na^+, K^+) diffuse internally and externally to balance membrane potential. At the same time, ion homeostasis is highly crucial for the energy-dependent transformation of cells and indispensable for maintaining cell growth. Thus, the electronegative phenolic compound noraucupatin may interfere with biological processes through electron transport and react with lipid proteins to attach to and destroy the outer membrane of bacteria.

5 Conclusion

In summary, the mechanism of action of a novel biphenyl compound noraucupatin against multidrug resistant *E. faecium* has been systematically and profoundly investigated by combining a variety of approaches. A series of thermodynamic parameters and the IC_{50} value (67.54 uM) determined that noraucupatin had an excellent bacteriostatic effect on the growth and metabolism of MDR *E. faecium*. Microscopic technical data revealed that noraucupatin leads to membrane rupture and death of MDR *E. faecium*. We consider that the mechanism of action of noraucupatin against MDR *E. faecium* is attributed to membrane rupture. Based on the analysis of the experimental data of membrane potential, membrane permeability and nuclear leakage, the membrane rupture is related to noraucupatin structure. Hydrophobic phenol groups accumulated in lipid bilayers and interact with lipid protein resulting changes of membrane structure stability, increasing membrane permeability causing the electrolyte disturbance of Na^+, K^+ ions, additionally lead to that accelerate the leakage of bacterial component. From the results of hemolytic activity tests, noraucupatin has been shown to have low cytotoxicity and excellent biocompatibility. The results presented here can provide a theoretical basis for the preparation of new antibiotics.

Data availability statement

The datasets used and/or analyzed during the current study are available from the corresponding author on reasonable request.

Author contributions

FY, experiment, investigation, methodology, visualization. X-LH, investigation, writing-original draft, writing-review and editing. JZ, LD, SL, Q-PL, and JY, formal analysis, investigation. YS, L-PG, and X-LY supervision, writing-review and editing.

Funding

This work was supported by Grants 32271538 (to X-LH), 81872755, 82073714 (to X-LY) from the National Natural Science Foundation of China and CZY23005 Fundamental Research Funds for South-Central Minzu University for Nationalities (X-LH) and 2060302-2101-20 (Q-PL) from China Academy of Chinese Medical Sciences and MZR20008 (to X-LY) from the National Civil Affairs Commission´s young and middle-aged talents training program.

Acknowledgments

We would like to thank the members of Wuhan Institute of Virology, Chinese Academy of Sciences for technical support.

Conflict of interest

The authors declare that the research was conducted in the absence of any commercial or financial relationships that could be construed as a potential conflict of interest.

Publisher's note

Supplementary material

The Supplementary Material for this article can be found online at: https://www.frontiersin.org/articles/10.3389/fchbi.2023.1181137/full#supplementary-material

References

Assis, L. R., Theodoro, R. D. S., Costa, M. B. S., Nascentes, J. A. S., Rocha, M. D. D., Bessa, M. A. d. S., et al. (2022). Antibacterial activity of isobavachalcone (IBC) is associated with membrane disruption. *Membr. (Basel)* 12, 269. doi:10.3390/membranes12030269

Bag, A., and Ghorai, P. K. (2016). Development of quantum chemical method to calculate half maximal inhibitory concentration (IC50). *Mol. Inf.* 35, 199–206. doi:10.1002/minf.201501004

Bhattacharya, D., Ghosh, D., Bhattacharya, S., Sarkar, S., Karmakar, P., Koley, H., et al. (2018). Antibacterial activity of polyphenolic fraction of kombucha against *Vibrio cholerae*: Targeting cell membrane. *Lett. Appl. Microbiol.* 66, 145–152. doi:10.1111/lam.12829

Bravo, D. (2022). Bacterial cadmium-immobilization activity measured by isothermal microcalorimetry in cacao-growing soils from Colombia. *Front. Environ. Sci.* 10. doi:10.3389/fenvs.2022.910234

Briaud, P., and Carroll, R. K. (2020). Extracellular vesicle biogenesis and functions in gram-positive bacteria. *Infect. Immun.* 88, e00433. doi:10.1128/IAI.00433-20

Carter, G. P., Harjani, J. R., Li, L., Pitcher, N. P., Nong, Y., Riley, T. V., et al. (2018). 1,2,4-Oxadiazole antimicrobials act synergistically with daptomycin and display rapid kill kinetics against MDR Enterococcus faecium. *J. Antimicrob. Chemother.* 73, 1562–1569. doi:10.1093/jac/dky064

Chen, Z., Xiong, Y., Tang, Y., Zhao, Y., Chen, J., Zheng, J., et al. (2022). *In vitro* activities of thiazolidione derivatives combined with daptomycin against clinical Enterococcus faecium strains. *BMC Microbiol.* 22, 16. doi:10.1186/s12866-021-02423-8

Cylke, C., Si, F., and Banerjee, S. (2022). Effects of antibiotics on bacterial cell morphology and their physiological origins. *Biochem. Soc. Trans.* 50, 1269–1279. doi:10.1042/BST20210894

da Silva, T. H., Hachigian, T. Z., Lee, J., and King, M. D. (2022). Using computers to ESKAPE the antibiotic resistance crisis. *Drug Discov. Today* 27, 456–470. doi:10.1016/j.drudis.2021.10.005

Dai, C., Lin, J., Li, H., Shen, Z., Wang, Y., Velkov, T., et al. (2022). The natural product curcumin as an antibacterial agent: Current achievements and problems. *Antioxidants (Basel)* 11, 459. doi:10.3390/antiox11030459

Dos Santos, G. R., Soeiro, V. S., Talarico, C. F., Ataide, J. A., Lopes, A. M., Mazzola, P. G., et al. (2022). Bacterial cellulose membranes as carriers for nisin: Incorporation, antimicrobial activity, cytotoxicity and morphology. *Polym. (Basel)* 14, 3497. doi:10.3390/polym14173497

El-Atrees, D. M., El-Kased, R. F., Abbas, A. M., and Yassien, M. A. (2022). Characterization and anti-biofilm activity of bacteriophages against urinary tract *Enterococcus faecalis* isolates. *Sci. Rep.* 12, 13048. doi:10.1038/s41598-022-17275-z

Fralliciardi, J., Melcr, J., Siginou, P., Marrink, S. J., and Poolman, B. (2022). Membrane thickness, lipid phase and sterol type are determining factors in the permeability of membranes to small solutes. *Nat. Commun.* 13, 1605. doi:10.1038/s41467-022-29272-x

Gao, Y., Yang, J., Yang, X. L., Zhang, L., Wang, J., Li, Q., et al. (2021). Novel dibenzofuran and biphenyl phytoalexins from Sorbus pohuashanensis suspension cell and their antimicrobial activities. *Fitoterapia* 152, 104914. doi:10.1016/j.fitote.2021.104914

Gregorchuk, B. S. J., Reimer, S. L., Slipski, C. J., Milner, K. A., Hiebert, S. L., Beniac, D. R., et al. (2022). Applying fluorescent dye assays to discriminate *Escherichia coli* chlorhexidine resistance phenotypes from porin and mlaA deletions and efflux pumps. *Sci. Rep.* 12, 12149. doi:10.1038/s41598-022-15775-6

Hajtuch, J., Santos-Martinez, M. J., Wojcik, M., Tomczyk, E., Jaskiewicz, M., Kamysz, W., et al. (2021). Lipoic acid-coated silver nanoparticles: Biosafety potential on the vascular microenvironment and antibacterial properties. *Front. Pharmacol.* 12, 733743. doi:10.3389/fphar.2021.733743

Hao, G., Shi, Y. H., Tang, Y. L., and Le, G. W. (2009). The membrane action mechanism of analogs of the antimicrobial peptide Buforin 2. *Peptides* 30, 1421–1427. doi:10.1016/j.peptides.2009.05.016

Jain, Z. J., Gide, P. S., and Kankate, R. S. (2017). Biphenyls and their derivatives as synthetically and pharmacologically important aromatic structural moieties. *Arabian J. Chem.* 10, S2051–S2066. doi:10.1016/j.arabjc.2013.07.035

Jia, D., Shen, F., Wang, Y., Wu, T., Xu, X., Zhang, X., et al. (2018). Apple fruit acidity is genetically diversified by natural variations in three hierarchical epistatic genes: MdSAUR37, MdPP2CH and MdALMTII. *Plant J.* 95, 427–443. doi:10.1111/tpj.13957

Kachur, K., and Suntres, Z. (2020). The antibacterial properties of phenolic isomers, carvacrol and thymol. *Crit. Rev. Food Sci. Nutr.* 60, 3042–3053. doi:10.1080/10408398.2019.1675585

Kessel, J., Bender, J., Werner, G., Griskaitis, M., Herrmann, E., Lehn, A., et al. (2021). Risk factors and outcomes associated with the carriage of tigecycline- and vancomycin-resistant. *J. Infect.* 82, 227–234. doi:10.1016/j.jinf.2020.12.003

Koh, J. J., Qiu, S., Zou, H., Lakshminarayanan, R., Li, J., Zhou, X., et al. (2013). Rapid bactericidal action of alpha-mangostin against MRSA as an outcome of membrane targeting. *Biochimica Biophysica Acta (BBA) - Biomembr.* 1828, 834–844. doi:10.1016/j.bbamem.2012.09.004

Lee, Y. S., Han, S. H., Lee, S. H., Kim, Y. G., Park, C. B., Kang, O. H., et al. (2012). The mechanism of antibacterial activity of tetrandrine against *Staphylococcus aureus*. *Foodborne Pathogens Dis.* 9, 686–691. doi:10.1089/fpd.2011.1119

Lesnichaya, M., Perfileva, A., Nozhkina, O., Gazizova, A., and Graskova, I. (2022). Synthesis, toxicity evaluation and determination of possible mechanisms of antimicrobial effect of arabinogalactane-capped selenium nanoparticles. *J. Trace Elem. Med. Biol.* 69, 126904. doi:10.1016/j.jtemb.2021.126904

Li, H., Li, Y., Wang, Y., Liu, L., Dong, H., and Satoh, T. (2022). Membrane-active amino acid-coupled polyetheramine derivatives with high selectivity and broad-spectrum antibacterial activity. *Acta Biomater.* 142, 136–148. doi:10.1016/j.actbio.2022.02.009

Li, Q., Chen, S., Zhu, K., Huang, X., Huang, Y., Shen, Z., et al. (2022). Collateral sensitivity to pleuromutilins in vancomycin-resistant Enterococcus faecium. *Nat. Commun.* 13, 1888. doi:10.1038/s41467-022-29493-0

Li, S., Zhan, J. K., Wang, Y. J., Lin, X., Zhong, J. Y., Wang, Y., et al. (2019). Exosomes from hyperglycemia-stimulated vascular endothelial cells contain versican that regulate calcification/senescence in vascular smooth muscle cells. *Cell Biosci.* 9, 1. doi:10.1186/s13578-018-0263-x

Lima, M. C., Paiva de Sousa, C., Fernandez-Prada, C., Harel, J., Dubreuil, J. D., and de Souza, E. L. (2019). A review of the current evidence of fruit phenolic compounds as potential antimicrobials against pathogenic bacteria. *Microb. Pathog.* 130, 259–270. doi:10.1016/j.micpath.2019.03.025

Mehta, D., Saini, V., Aggarwal, B., Khan, A., and Bajaj, A. (2021). Unlocking the bacterial membrane as a therapeutic target for next-generation antimicrobial amphiphiles. *Mol. Aspects Med.* 81, 100999. doi:10.1016/j.mam.2021.100999

Murray, C. J. L., Ikuta, K. S., Sharara, F., Swetschinski, L., Robles Aguilar, G., Gray, A., et al. (2022). Global burden of bacterial antimicrobial resistance in 2019: A systematic analysis. *Lancet* 399, 629–655. doi:10.1016/S0140-6736(21)02724-0

Nazir, S., Naz, T., Tahir, M. N., Rashid, M. A., Yaseen, M., and Whitwood, A. C. (2022). Crystallographic evidence of synthesized Ni(II) fluoride complex: Solubilization interaction of fluoride complex in anionic micellar media by conductometric and spectroscopic techniques. *J. Mol. Liq.* 348, 118042. doi:10.1016/j.molliq.2021.118042

Pisano, M., Dettori, M. A., Fabbri, D., Delogu, G., Palmieri, G., and Rozzo, C. (2021). Anticancer activity of two novel hydroxylated biphenyl compounds toward malignant melanoma cells. *Int. J. Mol. Sci.* 22, 5636. doi:10.3390/ijms22115636

Platon, V. M., Dragoi, B., and Marin, L. (2022). Erythromycin formulations-A journey to advanced drug delivery. *Pharmaceutics* 14, 2180. doi:10.3390/pharmaceutics14102180

Rajasekaran, G., Dinesh Kumar, S., Nam, J., Jeon, D., Kim, Y., Lee, C. W., et al. (2019). Antimicrobial and anti-inflammatory activities of chemokine CXCL14-derived antimicrobial peptide and its analogs. *Biochimica Biophysica Acta (BBA) - Biomembr.* 1861, 256–267. doi:10.1016/j.bbamem.2018.06.016

Ribeiro, P. R., Ferraz, C. G., Guedes, M. L., Martins, D., and Cruz, F. G. (2011). A new biphenyl and antimicrobial activity of extracts and compounds from Clusia burlemarxii. *Fitoterapia* 82, 1237–1240. doi:10.1016/j.fitote.2011.08.012

Ruhal, R., and Kataria, R. (2021). Biofilm patterns in gram-positive and gram-negative bacteria. *Microbiol. Res.* 251, 126829. doi:10.1016/j.micres.2021.126829

She, P., Liu, Y., Xu, L., Li, Y., Li, Z., Liu, S., et al. (2022). SPR741, double- or triple-combined with erythromycin and clarithromycin, combats drug-resistant *Klebsiella pneumoniae*, its biofilms, and persister cells. *Front. Cell Infect. Microbiol.* 12, 858606. doi:10.3389/fcimb.2022.858606

Sigg, A. P., Mariotti, M., Grutter, A. E., Lafranca, T., Leitner, L., Bonkat, G., et al. (2022). A method to determine the efficacy of a commercial phage preparation against uropathogens in urine and artificial urine determined by isothermal microcalorimetry. *Microorganisms* 10, 845. doi:10.3390/microorganisms10050845

Smith, T. T., Tamma, P. D., Do, T. B., Dzintars, K. E., Zhao, Y., Cosgrove, S. E., et al. (2018). Prolonged linezolid use is associated with the development of linezolid-resistant Enterococcus faecium. *Diagnostic Microbiol. Infect. Dis.* 91, 161–163. doi:10.1016/j.diagmicrobio.2018.01.027

Tague, A. J., Putsathit, P., Riley, T. V., Keller, P. A., and Pyne, S. G. (2021). Positional isomers of biphenyl antimicrobial peptidomimetic amphiphiles. *ACS Med. Chem. Lett.* 12, 413–419. doi:10.1021/acsmedchemlett.0c00611

Tan, S. C., Chong, C. W., Teh, C. S. J., Ooi, P. T., and Thong, K. L. (2018). Occurrence of virulent multidrug-resistant *Enterococcus faecalis* and Enterococcus faecium in the pigs, farmers and farm environments in Malaysia. *PeerJ* 6, e5353. doi:10.7717/peerj.5353

Tao, J., Yan, S., Zhou, C., Liu, Q., Zhu, H., and Wen, Z. (2021). Total flavonoids from Potentilla kleiniana Wight et Arn inhibits biofilm formation and virulence factors production in methicillin-resistant *Staphylococcus aureus* (MRSA). *J. Ethnopharmacol.* 279, 114383. doi:10.1016/j.jep.2021.114383

Tran, T. T., Munita, J. M., and Arias, C. A. (2015). Mechanisms of drug resistance: Daptomycin resistance. *Ann. N. Y. Acad. Sci.* 1354, 32–53. doi:10.1111/nyas.12948

Wu, Y., Bai, J., Zhong, K., Huang, Y., Qi, H., Jiang, Y., et al. (2016). Antibacterial activity and membrane-disruptive mechanism of 3-p-trans-Coumaroyl-2-hydroxyquinic acid, a novel phenolic compound from pine needles of cedrus deodara, against *Staphylococcus aureus*. *Molecules* 21, 1084. doi:10.3390/molecules21081084

Yi, M., Zou, J., Zhao, J., Tang, Y., Yuan, Y., Yang, B., et al. (2022). Emergence of optrA-mediated linezolid resistance in Enterococcus faecium: A molecular investigation in a tertiary hospital of southwest China from 2014-2018. *Infect. Drug Resist.* 15, 13–20. doi:10.2147/IDR.S339761

Zhang, F., and Cheng, W. (2022). The mechanism of bacterial resistance and potential bacteriostatic strategies. *Antibiot. (Basel)* 11, 1215. doi:10.3390/antibiotics11091215

Zhang, X., Han, D., Pei, P., Hao, J., Lu, Y., Wan, P., et al. (2019). <p>*in vitro* Antibacterial Activity of Isopropoxy Benzene Guanidine against Multidrug-Resistant Enterococci</p>. *Infect. Drug Resist.* 12, 3943–3953. doi:10.2147/IDR.S234509

Zhou, Q., Si, Z., Wang, K., Li, K., Hong, W., Zhang, Y., et al. (2022). Enzyme-triggered smart antimicrobial drug release systems against bacterial infections. *J. Control. Release* 352, 507–526. doi:10.1016/j.jconrel.2022.10.038